

A Search for the Rare Decay $B^0 \rightarrow \tau^+\tau^-$ at *BABAR*

B. Aubert,¹ R. Barate,¹ D. Boutigny,¹ F. Couderc,¹ Y. Karyotakis,¹ J. P. Lees,¹ V. Poireau,¹ V. Tisserand,¹
A. Zghiche,¹ E. Grauges,² A. Palano,³ M. Pappagallo,³ A. Pompili,³ J. C. Chen,⁴ N. D. Qi,⁴ G. Rong,⁴ P. Wang,⁴
Y. S. Zhu,⁴ G. Eigen,⁵ I. Ofte,⁵ B. Stugu,⁵ G. S. Abrams,⁶ M. Battaglia,⁶ A. B. Breon,⁶ D. N. Brown,⁶
J. Button-Shafer,⁶ R. N. Cahn,⁶ E. Charles,⁶ C. T. Day,⁶ M. S. Gill,⁶ A. V. Gritsan,⁶ Y. Groysman,⁶
R. G. Jacobsen,⁶ R. W. Kadel,⁶ J. Kadyk,⁶ L. T. Kerth,⁶ Yu. G. Kolomensky,⁶ G. Kukartsev,⁶ G. Lynch,⁶
L. M. Mir,⁶ P. J. Oddone,⁶ T. J. Orimoto,⁶ M. Pripstein,⁶ N. A. Roe,⁶ M. T. Ronan,⁶ W. A. Wenzel,⁶ M. Barrett,⁷
K. E. Ford,⁷ T. J. Harrison,⁷ A. J. Hart,⁷ C. M. Hawkes,⁷ S. E. Morgan,⁷ A. T. Watson,⁷ M. Fritsch,⁸ K. Goetzen,⁸
T. Held,⁸ H. Koch,⁸ B. Lewandowski,⁸ M. Pelzaeus,⁸ K. Peters,⁸ T. Schroeder,⁸ M. Steinke,⁸ J. T. Boyd,⁹
J. P. Burke,⁹ N. Chevalier,⁹ W. N. Cottingham,⁹ T. Cuhadar-Donszelmann,¹⁰ B. G. Fulsom,¹⁰ C. Hearty,¹⁰
N. S. Knecht,¹⁰ T. S. Mattison,¹⁰ J. A. McKenna,¹⁰ A. Khan,¹¹ P. Kyberd,¹¹ M. Saleem,¹¹ L. Teodorescu,¹¹
A. E. Blinov,¹² V. E. Blinov,¹² A. D. Bukin,¹² V. P. Druzhinin,¹² V. B. Golubev,¹² E. A. Kravchenko,¹²
A. P. Onuchin,¹² S. I. Serednyakov,¹² Yu. I. Skovpen,¹² E. P. Solodov,¹² A. N. Yushkov,¹² D. Best,¹³ M. Bondioli,¹³
M. Bruinsma,¹³ M. Chao,¹³ S. Curry,¹³ I. Eschrich,¹³ D. Kirkby,¹³ A. J. Lankford,¹³ P. Lund,¹³ M. Mandelkern,¹³
R. K. Mommsen,¹³ W. Roethel,¹³ D. P. Stoker,¹³ C. Buchanan,¹⁴ B. L. Hartfiel,¹⁴ A. J. R. Weinstein,¹⁴
S. D. Foulkes,¹⁵ J. W. Gary,¹⁵ O. Long,¹⁵ B. C. Shen,¹⁵ K. Wang,¹⁵ L. Zhang,¹⁵ D. del Re,¹⁶ H. K. Hadavand,¹⁶
E. J. Hill,¹⁶ D. B. MacFarlane,¹⁶ H. P. Paar,¹⁶ S. Rahatlou,¹⁶ V. Sharma,¹⁶ J. W. Berryhill,¹⁷ C. Campagnari,¹⁷
A. Cunha,¹⁷ B. Dahmes,¹⁷ T. M. Hong,¹⁷ M. A. Mazur,¹⁷ J. D. Richman,¹⁷ W. Verkerke,¹⁷ T. W. Beck,¹⁸
A. M. Eisner,¹⁸ C. J. Flacco,¹⁸ C. A. Heusch,¹⁸ J. Kroseberg,¹⁸ W. S. Lockman,¹⁸ G. Nesom,¹⁸ T. Schalk,¹⁸
B. A. Schumm,¹⁸ A. Seiden,¹⁸ P. Spradlin,¹⁸ D. C. Williams,¹⁸ M. G. Wilson,¹⁸ J. Albert,¹⁹ E. Chen,¹⁹
G. P. Dubois-Felsmann,¹⁹ A. Dvoretzki,¹⁹ D. G. Hitlin,¹⁹ I. Narsky,¹⁹ T. Piatenko,¹⁹ F. C. Porter,¹⁹ A. Ryd,¹⁹
A. Samuel,¹⁹ R. Andreassen,²⁰ G. Mancinelli,²⁰ B. T. Meadows,²⁰ M. D. Sokoloff,²⁰ F. Blanc,²¹ P. Bloom,²¹
S. Chen,²¹ W. T. Ford,²¹ J. F. Hirschauer,²¹ A. Kreisel,²¹ U. Nauenberg,²¹ A. Olivas,²¹ P. Rankin,²¹
W. O. Ruddick,²¹ J. G. Smith,²¹ K. A. Ulmer,²¹ S. R. Wagner,²¹ J. Zhang,²¹ A. Chen,²² E. A. Eckhart,²²
J. L. Harton,²² A. Soffer,²² W. H. Toki,²² R. J. Wilson,²² Q. Zeng,²² R. Aleksan,²³ S. Emery,²³ A. Gaidot,²³
S. F. Ganzhur,²³ P.-F. Giraud,²³ G. Graziani,²³ G. Hamel de Monchenault,²³ W. Kozanecki,²³ M. Legendre,²³
G. W. London,²³ B. Mayer,²³ G. Vasseur,²³ Ch. Yeche,²³ M. Zito,²³ D. Altenburg,²⁴ E. Feltresi,²⁴ A. Hauke,²⁴
B. Spaan,²⁴ T. Brandt,²⁵ J. Brose,²⁵ M. Dickopp,²⁵ V. Klose,²⁵ H. M. Lacker,²⁵ R. Nogowski,²⁵ S. Otto,²⁵
A. Petzold,²⁵ J. Schubert,²⁵ K. R. Schubert,²⁵ R. Schwierz,²⁵ J. E. Sundermann,²⁵ D. Bernard,²⁶ G. R. Bonneaud,²⁶
P. Grenier,²⁶ S. Schrenk,²⁶ Ch. Thiebaux,²⁶ G. Vasileiadis,²⁶ M. Verderi,²⁶ D. J. Bard,²⁷ P. J. Clark,²⁷ W. Gradl,²⁷
F. Muheim,²⁷ S. Playfer,²⁷ Y. Xie,²⁷ M. Andreotti,²⁸ V. Azzolini,²⁸ D. Bettoni,²⁸ C. Bozzi,²⁸ R. Calabrese,²⁸
G. Cibinetto,²⁸ E. Lippi,²⁸ M. Negrini,²⁸ L. Piemontese,²⁸ F. Anulli,²⁹ R. Baldini-Ferrolli,²⁹ A. Calcaterra,²⁹ R. de
Sangro,²⁹ G. Finocchiaro,²⁹ P. Patteri,²⁹ I. M. Peruzzi,²⁹ M. Piccolo,²⁹ A. Zallo,²⁹ A. Buzzo,³⁰ R. Capra,³⁰
R. Contri,³⁰ M. Lo Vetere,³⁰ M. Macri,³⁰ M. R. Monge,³⁰ S. Passaggio,³⁰ C. Patrignani,³⁰ E. Robutti,³⁰
A. Santroni,³⁰ S. Tosi,³⁰ G. Brandenburg,³¹ K. S. Chaisanguanthum,³¹ M. Morii,³¹ E. Won,³¹ J. Wu,³¹
R. S. Dubitzky,³² U. Langenegger,³² J. Marks,³² S. Schenk,³² U. Uwer,³² F. Martinez-Vidal,³³ W. Bhimji,³⁴
D. A. Bowerman,³⁴ P. D. Dauncey,³⁴ U. Egede,³⁴ R. L. Flack,³⁴ J. R. Gaillard,³⁴ G. W. Morton,³⁴ J. A. Nash,³⁴
M. B. Nikolich,³⁴ G. P. Taylor,³⁴ W. P. Vazquez,³⁴ M. J. Charles,³⁵ W. F. Mader,³⁵ U. Mallik,³⁵ A. K. Mohapatra,³⁵
J. Cochran,³⁶ H. B. Crawley,³⁶ V. Eyges,³⁶ W. T. Meyer,³⁶ S. Prell,³⁶ E. I. Rosenberg,³⁶ A. E. Rubin,³⁶ J. Yi,³⁶
M. Biasini,³⁷ R. Covarelli,³⁷ S. Pacetti,³⁷ M. Pioppi,³⁷ N. Arnaud,³⁸ M. Davier,³⁸ X. Giroux,³⁸ G. Grosdidier,³⁸
A. Höcker,³⁸ F. Le Diberder,³⁸ V. Lepeltier,³⁸ A. M. Lutz,³⁸ A. Oyanguren,³⁸ T. C. Petersen,³⁸ M. Pierini,³⁸
S. Plaszczynski,³⁸ S. Rodier,³⁸ P. Roudeau,³⁸ M. H. Schune,³⁸ A. Stocchi,³⁸ G. Wormser,³⁸ C. H. Cheng,³⁹
D. J. Lange,³⁹ M. C. Simani,³⁹ D. M. Wright,³⁹ A. J. Bevan,⁴⁰ C. A. Chavez,⁴⁰ Ian J. Forster,⁴⁰ J. R. Fry,⁴⁰
E. Gabathuler,⁴⁰ R. Gamet,⁴⁰ K. A. George,⁴⁰ D. E. Hutchcroft,⁴⁰ R. J. Parry,⁴⁰ D. J. Payne,⁴⁰ K. C. Schofield,⁴⁰

C. Touramanis,⁴⁰ C. M. Cormack,⁴¹ F. Di Lodovico,⁴¹ W. Menges,⁴¹ R. Sacco,⁴¹ C. L. Brown,⁴² G. Cowan,⁴² H. U. Flaecher,⁴² M. G. Green,⁴² D. A. Hopkins,⁴² P. S. Jackson,⁴² T. R. McMahon,⁴² S. Ricciardi,⁴² F. Salvatore,⁴² D. Brown,⁴³ C. L. Davis,⁴³ J. Allison,⁴⁴ N. R. Barlow,⁴⁴ R. J. Barlow,⁴⁴ C. L. Edgar,⁴⁴ M. C. Hodgkinson,⁴⁴ M. P. Kelly,⁴⁴ G. D. Lafferty,⁴⁴ M. T. Naisbit,⁴⁴ J. C. Williams,⁴⁴ C. Chen,⁴⁵ W. D. Hulsbergen,⁴⁵ A. Jawahery,⁴⁵ D. Kovalskyi,⁴⁵ C. K. Lae,⁴⁵ D. A. Roberts,⁴⁵ G. Simi,⁴⁵ G. Blaylock,⁴⁶ C. Dallapiccola,⁴⁶ S. S. Hertzbach,⁴⁶ R. Kofler,⁴⁶ V. B. Koptchev,⁴⁶ X. LI,⁴⁶ T. B. Moore,⁴⁶ S. Saremi,⁴⁶ H. Staengle,⁴⁶ S. Willocq,⁴⁶ R. Cowan,⁴⁷ K. Koeneke,⁴⁷ G. Sciolla,⁴⁷ S. J. Sekula,⁴⁷ M. Spitznagel,⁴⁷ F. Taylor,⁴⁷ R. K. Yamamoto,⁴⁷ H. Kim,⁴⁸ P. M. Patel,⁴⁸ S. H. Robertson,⁴⁸ A. Lazzaro,⁴⁹ V. Lombardo,⁴⁹ F. Palombo,⁴⁹ J. M. Bauer,⁵⁰ L. Cremaldi,⁵⁰ V. Eschenburg,⁵⁰ R. Godang,⁵⁰ R. Kroeger,⁵⁰ J. Reidy,⁵⁰ D. A. Sanders,⁵⁰ D. J. Summers,⁵⁰ H. W. Zhao,⁵⁰ S. Brunet,⁵¹ D. Cote,⁵¹ P. Taras,⁵¹ B. Viaud,⁵¹ H. Nicholson,⁵² M. Baak,⁵³ H. Bulten,⁵³ G. Raven,⁵³ H. L. Snoek,⁵³ L. Wilden,⁵³ N. Cavallo,⁵⁴ G. De Nardo,⁵⁴ F. Fabozzi,⁵⁴ C. Gatto,⁵⁴ L. Lista,⁵⁴ D. Monorchio,⁵⁴ P. Paolucci,⁵⁴ D. Piccolo,⁵⁴ C. Sciacca,⁵⁴ C. P. Jessop,⁵⁵ J. M. LoSecco,⁵⁵ T. Allmendinger,⁵⁶ G. Benelli,⁵⁶ K. K. Gan,⁵⁶ K. Honscheid,⁵⁶ D. Hufnagel,⁵⁶ P. D. Jackson,⁵⁶ H. Kagan,⁵⁶ R. Kass,⁵⁶ T. Pulliam,⁵⁶ A. M. Rahimi,⁵⁶ R. Ter-Antonyan,⁵⁶ Q. K. Wong,⁵⁶ J. Brau,⁵⁷ R. Frey,⁵⁷ O. Igonkina,⁵⁷ M. LU,⁵⁷ C. T. Potter,⁵⁷ N. B. Sinev,⁵⁷ D. Strom,⁵⁷ J. Strube,⁵⁷ E. Torrence,⁵⁷ F. Galeazzi,⁵⁸ M. Margoni,⁵⁸ M. Morandin,⁵⁸ M. Posocco,⁵⁸ M. Rotondo,⁵⁸ F. Simonetto,⁵⁸ R. Stroili,⁵⁸ C. Voci,⁵⁸ M. Benayoun,⁵⁹ H. Briand,⁵⁹ J. Chauveau,⁵⁹ P. David,⁵⁹ C. de la Vaissiere,⁵⁹ L. Del Buono,⁵⁹ O. Hamon,⁵⁹ M. J. J. John,⁵⁹ Ph. Leruste,⁵⁹ J. Malcles,⁵⁹ J. Ocariz,⁵⁹ L. Roos,⁵⁹ G. Therin,⁵⁹ P. K. Behera,⁶⁰ L. Gladney,⁶⁰ Q. H. Guo,⁶⁰ J. Panetta,⁶⁰ C. Angelini,⁶¹ G. Batignani,⁶¹ S. Bettarini,⁶¹ F. Bucci,⁶¹ G. Calderini,⁶¹ M. Carpinelli,⁶¹ R. Cenci,⁶¹ F. Forti,⁶¹ M. A. Giorgi,⁶¹ A. Lusiani,⁶¹ G. Marchiori,⁶¹ M. Morganit,⁶¹ N. Neri,⁶¹ E. Paoloni,⁶¹ M. Rama,⁶¹ G. Rizzo,⁶¹ J. Walsh,⁶¹ M. Haire,⁶² D. Judd,⁶² D. E. Wagoner,⁶² J. Biesiada,⁶³ N. Danielson,⁶³ P. Elmer,⁶³ Y. Lau,⁶³ C. Lu,⁶³ J. Olsen,⁶³ A. J. S. Smith,⁶³ A. V. Telnov,⁶³ F. Bellini,⁶⁴ G. Cavoto,⁶⁴ A. D’Orazio,⁶⁴ E. Di Marco,⁶⁴ R. Faccini,⁶⁴ * F. Ferrarotto,⁶⁴ F. Ferroni,⁶⁴ M. Gaspero,⁶⁴ L. Li Gioi,⁶⁴ M. A. Mazzoni,⁶⁴ S. Morganti,⁶⁴ G. Piredda,⁶⁴ F. Polci,⁶⁴ F. Safai Tehrani,⁶⁴ C. Voena,⁶⁴ H. Schröder,⁶⁵ G. Wagner,⁶⁵ R. Waldi,⁶⁵ T. Adye,⁶⁶ N. De Groot,⁶⁶ B. Franek,⁶⁶ G. P. Gopal,⁶⁶ E. O. Olaiya,⁶⁶ F. F. Wilson,⁶⁶ M. V. Purohit,⁶⁷ A. W. Weidemann,⁶⁷ J. R. Wilson,⁶⁷ F. X. Yumiceva,⁶⁷ T. Abe,⁶⁸ M. T. Allen,⁶⁸ D. Aston,⁶⁸ R. Bartoldus,⁶⁸ N. Berger,⁶⁸ A. M. Boyarski,⁶⁸ O. L. Buchmueller,⁶⁸ R. Claus,⁶⁸ J. P. Coleman,⁶⁸ M. R. Convery,⁶⁸ M. Cristinziani,⁶⁸ J. C. Dingfelder,⁶⁸ D. Dong,⁶⁸ J. Dorfan,⁶⁸ D. Dujmic,⁶⁸ W. Dunwoodie,⁶⁸ S. Fan,⁶⁸ R. C. Field,⁶⁸ T. Glanzman,⁶⁸ S. J. Gowdy,⁶⁸ T. Hadig,⁶⁸ V. Halyo,⁶⁸ C. Hast,⁶⁸ T. Hryn’ova,⁶⁸ W. R. Innes,⁶⁸ M. H. Kelsey,⁶⁸ P. Kim,⁶⁸ M. L. Kocian,⁶⁸ D. W. G. S. Leith,⁶⁸ J. Libby,⁶⁸ S. Luitz,⁶⁸ V. Luth,⁶⁸ H. L. Lynch,⁶⁸ H. Marsiske,⁶⁸ R. Messner,⁶⁸ D. R. Muller,⁶⁸ C. P. O’Grady,⁶⁸ V. E. Ozcan,⁶⁸ A. Perazzo,⁶⁸ M. Perl,⁶⁸ B. N. Ratcliff,⁶⁸ A. Roodman,⁶⁸ A. A. Salnikov,⁶⁸ R. H. Schindler,⁶⁸ J. Schwiening,⁶⁸ A. Snyder,⁶⁸ J. Stelzer,⁶⁸ D. Su,⁶⁸ M. K. Sullivan,⁶⁸ K. Suzuki,⁶⁸ S. K. Swain,⁶⁸ J. M. Thompson,⁶⁸ J. Va’vra,⁶⁸ N. van Bakel,⁶⁸ M. Weaver,⁶⁸ W. J. Wisniewski,⁶⁸ M. Wittgen,⁶⁸ D. H. Wright,⁶⁸ A. K. Yarritu,⁶⁸ K. Yi,⁶⁸ C. C. Young,⁶⁸ P. R. Burchat,⁶⁹ A. J. Edwards,⁶⁹ S. A. Majewski,⁶⁹ B. A. Petersen,⁶⁹ C. Roat,⁶⁹ M. Ahmed,⁷⁰ S. Ahmed,⁷⁰ M. S. Alam,⁷⁰ R. BULA,⁷⁰ J. A. Ernst,⁷⁰ M. A. Saeed,⁷⁰ F. R. Wappler,⁷⁰ S. B. Zain,⁷⁰ W. Bugg,⁷¹ M. Krishnamurthy,⁷¹ S. M. Spanier,⁷¹ R. Eckmann,⁷² J. L. Ritchie,⁷² A. Satpathy,⁷² R. F. Schwitters,⁷² J. M. Izen,⁷³ I. Kitayama,⁷³ X. C. Lou,⁷³ S. Ye,⁷³ F. Bianchi,⁷⁴ M. Bona,⁷⁴ F. Gallo,⁷⁴ D. Gamba,⁷⁴ M. Bomben,⁷⁵ L. Bosisio,⁷⁵ C. Cartaro,⁷⁵ F. Cossutti,⁷⁵ G. Della Ricca,⁷⁵ S. Dittongo,⁷⁵ S. Grancagnolo,⁷⁵ L. Lanceri,⁷⁵ L. Vitale,⁷⁵ R. S. Panvini,⁷⁶ Sw. Banerjee,⁷⁷ B. Bhuyan,⁷⁷ C. M. Brown,⁷⁷ D. Fortin,⁷⁷ K. Hamano,⁷⁷ R. Kowalewski,⁷⁷ J. M. Roney,⁷⁷ R. J. Sobie,⁷⁷ J. J. Back,⁷⁸ P. F. Harrison,⁷⁸ T. E. Latham,⁷⁸ G. B. Mohanty,⁷⁸ H. R. Band,⁷⁹ X. Chen,⁷⁹ B. Cheng,⁷⁹ S. Dasu,⁷⁹ M. Datta,⁷⁹ A. M. Eichenbaum,⁷⁹ K. T. Flood,⁷⁹ M. Graham,⁷⁹ J. J. Hollar,⁷⁹ J. R. Johnson,⁷⁹ P. E. Kutter,⁷⁹ H. Li,⁷⁹ R. Liu,⁷⁹ B. Mellado,⁷⁹ A. Mihalysi,⁷⁹ Y. Pan,⁷⁹ R. Prepost,⁷⁹ P. Tan,⁷⁹ J. H. von Wimmersperg-Toeller,⁷⁹ S. L. Wu,⁷⁹ Z. Yu,⁷⁹ H. Neal,⁸⁰ and G. Schott⁸¹

(The BABAR Collaboration)

¹Laboratoire de Physique des Particules, F-74941 Annecy-le-Vieux, France

²Universitat de Barcelona (IFAE) Fac. Fisica. Dept. ECM Avda Diagonal 647, 6a planta E-08028 Barcelona, Spain

³Università di Bari, Dipartimento di Fisica and INFN, I-70126 Bari, Italy

⁴Institute of High Energy Physics, Beijing 100039, China

⁵University of Bergen, Inst. of Physics, N-5007 Bergen, Norway

⁶Lawrence Berkeley National Laboratory and University of California, Berkeley, CA 94720, USA

⁷University of Birmingham, Birmingham, B15 2TT, United Kingdom

⁸Ruhr Universität Bochum, Institut für Experimentalphysik 1, D-44780 Bochum, Germany

⁹University of Bristol, Bristol BS8 1TL, United Kingdom

- ¹⁰ University of British Columbia, Vancouver, BC, Canada V6T 1Z1
- ¹¹ Brunel University, Uxbridge, Middlesex UB8 3PH, United Kingdom
- ¹² Budker Institute of Nuclear Physics, Novosibirsk 630090, Russia
- ¹³ University of California at Irvine, Irvine, CA 92697, USA
- ¹⁴ University of California at Los Angeles, Los Angeles, CA 90024, USA
- ¹⁵ Univ. of California, Riverside, CA 92521
- ¹⁶ University of California at San Diego, La Jolla, CA 92093, USA
- ¹⁷ University of California at Santa Barbara, Santa Barbara, CA 93106, USA
- ¹⁸ University of California at Santa Cruz, Institute for Particle Physics, Santa Cruz, CA 95064, USA
- ¹⁹ California Institute of Technology, Pasadena, CA 91125, USA
- ²⁰ University of Cincinnati, Cincinnati, OH 45221, USA
- ²¹ University of Colorado, Boulder, CO 80309, USA
- ²² Colorado State University, Fort Collins, CO 80523, USA
- ²³ DSM/Dapnia, CEA/Saclay, F-91191 Gif-sur-Yvette, France
- ²⁴ Universität Dortmund, Institut für Physik, D-44221 Dortmund, Germany
- ²⁵ Technische Universität Dresden, Institut für Kern- und Teilchenphysik, D-01062 Dresden, Germany
- ²⁶ Ecole Polytechnique, LLR, F-91128 Palaiseau, France
- ²⁷ University of Edinburgh, Edinburgh EH9 3JZ, United Kingdom
- ²⁸ Università di Ferrara, Dipartimento di Fisica and INFN, I-44100 Ferrara, Italy
- ²⁹ Laboratori Nazionali di Frascati dell'INFN, I-00044 Frascati, Italy
- ³⁰ Università di Genova, Dipartimento di Fisica and INFN, I-16146 Genova, Italy
- ³¹ Harvard University, Cambridge, MA 02138, USA
- ³² Univ. Heidelberg, Philosophenweg 12, D-69120 Heidelberg, Germany
- ³³ IFIC, Universitat de Valencia - CSIC, Apdo. 22085, E-46071 Valencia, Spain
- ³⁴ Imperial College London, London, SW7 2AZ, United Kingdom
- ³⁵ University of Iowa, Iowa City, IA 52242, USA
- ³⁶ Iowa State University, Ames, IA 50011-3160, USA
- ³⁷ Istituto Naz. Fis. Nucleare, I-06100 Perugia, Italy
- ³⁸ Laboratoire de l'Accélérateur Linéaire, F-91898 Orsay, France
- ³⁹ Lawrence Livermore National Laboratory, Livermore, CA 94550, USA
- ⁴⁰ University of Liverpool, Liverpool L69 7ZE, United Kingdom
- ⁴¹ Queen Mary, University of London, E1 4NS, United Kingdom
- ⁴² University of London, Royal Holloway and Bedford New College, Egham, Surrey TW20 0EX, United Kingdom
- ⁴³ University of Louisville, Louisville, KY 40292, USA
- ⁴⁴ University of Manchester, Manchester M13 9PL, United Kingdom
- ⁴⁵ University of Maryland, College Park, MD 20742, USA
- ⁴⁶ University of Massachusetts, Amherst, MA 01003, USA
- ⁴⁷ Massachusetts Institute of Technology, Laboratory for Nuclear Science, Cambridge, MA 02139, USA
- ⁴⁸ McGill University, Montréal, QC, Canada H3A 2T8
- ⁴⁹ Università di Milano, Dipartimento di Fisica and INFN, I-20133 Milano, Italy
- ⁵⁰ University of Mississippi, University, MS 38677, USA
- ⁵¹ Université de Montréal, Laboratoire René J. A. Lévesque, Montréal, QC, Canada H3C 3J7
- ⁵² Mount Holyoke College, South Hadley, MA 01075, USA
- ⁵³ NIKHEF, National Institute for Nuclear Physics and High Energy Physics, NL-1009 DB Amsterdam, The Netherlands
- ⁵⁴ Università di Napoli Federico II, Dipartimento di Scienze Fisiche and INFN, I-80126, Napoli, Italy
- ⁵⁵ University of Notre Dame, Notre Dame, IN 46556, USA
- ⁵⁶ Ohio State University, Columbus, OH 43210, USA
- ⁵⁷ University of Oregon, Eugene, OR 97403, USA
- ⁵⁸ Università di Padova, Dipartimento di Fisica and INFN, I-35131 Padova, Italy
- ⁵⁹ Universités Paris VI et VII, Lab de Physique Nucléaire H. E., F-75252 Paris, France
- ⁶⁰ University of Pennsylvania, Philadelphia, PA 19104, USA
- ⁶¹ Università di Pisa, Dipartimento di Fisica, Scuola Normale Superiore and INFN, I-56127 Pisa, Italy
- ⁶² Prairie View A&M University, Prairie View, TX 77446, USA
- ⁶³ Princeton University, Princeton, NJ 08544, USA
- ⁶⁴ Università di Roma La Sapienza, Dipartimento di Fisica and INFN, I-00185 Roma, Italy
- ⁶⁵ Universität Rostock, D-18051 Rostock, Germany
- ⁶⁶ Rutherford Appleton Laboratory, Chilton, Didcot, Oxon, OX11 0QX, United Kingdom
- ⁶⁷ University of South Carolina, Columbia, SC 29208, USA
- ⁶⁸ Stanford Linear Accelerator Center, Stanford, CA 94309, USA
- ⁶⁹ Stanford University, Stanford, CA 94305-4060, USA
- ⁷⁰ State Univ. of New York, Albany, NY 12222, USA
- ⁷¹ University of Tennessee, Knoxville, TN 37996, USA
- ⁷² University of Texas at Austin, Austin, TX 78712, USA
- ⁷³ University of Texas at Dallas, Richardson, TX 75083, USA

⁷⁴Università di Torino, Dipartimento di Fisica Sperimentale and INFN, I-10125 Torino, Italy

⁷⁵Università di Trieste, Dipartimento di Fisica and INFN, I-34127 Trieste, Italy

⁷⁶Vanderbilt University, Nashville, TN 37235, USA

⁷⁷University of Victoria, Victoria, BC, Canada V8W 3P6

⁷⁸Univ. of Warwick, Coventry, Warwicks. CV4 7AL, England

⁷⁹University of Wisconsin, Madison, WI 53706, USA

⁸⁰Yale University, New Haven, CT 06511, USA

⁸¹Institut fuer Experimentelle Kernphysik (IEKP) University of Karlsruhe Postfach 3640 D-76021 Karlsruhe Germany

(Dated: June 29, 2006)

We present the results of a search for the decay $B^0 \rightarrow \tau^+\tau^-$ in a data sample of $(232 \pm 3) \times 10^6$ $\Upsilon(4S) \rightarrow B\bar{B}$ decays using the BABAR detector. Certain extensions of the Standard Model predict measurable levels of this otherwise rare decay. We reconstruct fully one neutral B meson and seek evidence for the signal decay in the rest of the event. We find no evidence for signal events and obtain $\mathcal{B}(B^0 \rightarrow \tau^+\tau^-) < 3.2 \times 10^{-3}$ at the 90% confidence level.

PACS numbers: 13.20.He, 14.40.Nd, 14.60.Fg

None of the leptonic decays $B^0 \rightarrow \ell^+\ell^-$ ($\ell = e, \mu, \tau$) have been observed. In the standard model of particle physics, the decays can be mediated by box and penguin diagrams (Fig. 1). The standard model produces only the combinations $\ell_R^+\ell_L^-$ and $\ell_L^+\ell_R^-$. The amplitudes for the decay of a spin-zero particle to these states are proportional to m_ℓ and thus the decay rates are suppressed by $(m_\ell/m_B)^2$. The suppression is smallest for $B^0 \rightarrow \tau^+\tau^-$ due to the large τ mass. The standard model prediction for the $B^0 \rightarrow \tau^+\tau^-$ branching fraction is [1]

$$\mathcal{B}^{SM}(B^0 \rightarrow \tau^+\tau^-) = 1.2 \times 10^{-7} \times \left[\frac{f_B}{200 \text{ MeV}} \right]^2 \left[\frac{|V_{td}|}{0.007} \right]^2, \quad (1)$$

where f_B is the B decay constant and V_{td} is the Cabibbo-Kobayashi-Maskawa matrix element. The theoretical uncertainty on f_B and the experimental error on V_{td} dominate the uncertainty on the predicted branching fraction.

Extensions of the standard model containing leptoquarks, which couple leptons to quarks, predict enhancements for $\mathcal{B}(B^0 \rightarrow \tau^+\tau^-)$ [2] that are proportional to the square of the leptoquark coupling. In theories that contain two Higgs doublet fields, the rate can be enhanced by powers of $\tan \beta$, the ratio of vacuum expectation values of the two Higgs doublet fields [3, 4]. Since $B^0 \rightarrow \ell^+\ell^-$ has not been observed, one can only constrain model parameters using the measured branching fraction limits. While $\tan \beta$ is constrained by all three modes ($\ell = e, \mu, \tau$), only $B^0 \rightarrow \tau^+\tau^-$ can constrain the coupling of a leptoquark to the third lepton generation or other new physics involving only the third generation.

The analysis described here provides the first upper limit on $\mathcal{B}(B^0 \rightarrow \tau^+\tau^-)$. The data were collected with the BABAR detector at the asymmetric PEP-II e^+e^- storage ring. A full description of the BABAR detector is given in Ref. [5]. In brief, charged-particle momenta are measured with a tracking system comprising a silicon vertex detector (SVT) and a drift chamber (DCH) placed

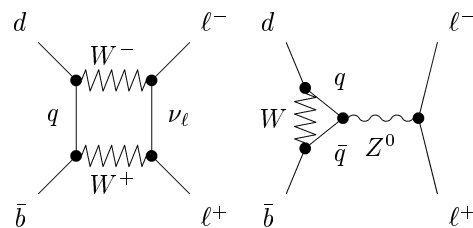


FIG. 1: Standard model box and penguin processes that can mediate $B^0 \rightarrow \ell^+\ell^-$ ($q = t, c, u$).

within a highly uniform 1.5-T magnetic field generated by a superconducting solenoid. Electron and photon energies are measured with an electromagnetic calorimeter (EMC) constructed with Thallium-doped CsI scintillating crystals. Muons are distinguished from hadrons in a steel magnetic-flux return instrumented with resistive plate chambers (IFR). Charged particle identification is provided by a Cherenkov detector (DIRC) and the tracking system. The data sample consists of 210 fb^{-1} collected at the peak of the $\Upsilon(4S)$ resonance, which corresponds to 232 ± 3 million $B\bar{B}$ pairs. The expected background and the expected signal efficiency are obtained from Monte Carlo simulation samples. The sample events were generated with the EvtGen event simulator [6] and propagated through a detailed model of the BABAR detector using the GEANT4 detector simulator [7].

Isolating $B^0 \rightarrow \tau^+\tau^-$ poses a unique challenge. This decay contains at least two and as many as four neutrinos, so there is no kinematic discriminant that separates signal from background due to undetected particles. Since two B mesons are produced in an $\Upsilon(4S)$ decay, the misassignment of decay products to the parent B must be avoided. We completely reconstruct one B candidate in each event (hereafter referred to as the companion B) and search for the signal decay among the remaining detected particles. The combinatorial background in the companion- B reconstruction is determined by a fit to

the companion- B invariant mass distribution. We employ the parameters

$$m_{\text{ES}} = \sqrt{E_{\text{beam}}^{*2} - p_B^{*2}} \quad (2)$$

$$\Delta E = E_B^* - E_{\text{beam}}^*, \quad (3)$$

where p_B^* and E_B^* are the reconstructed companion- B momentum and energy in the center-of-mass (CM) frame. E_{beam}^* is the beam energy in the CM frame. The m_{ES} distributions are fit with a probability density function composed of a Crystal Ball function [8] to model the peak at the B mass and an ARGUS function [9] to model the nonpeaking combinatorial background.

The companion B is fully reconstructed in a hadronic mode $\bar{B}^0 \rightarrow D^{(*)}X$, where $D^{(*)}$ is either a D^+ [10], D^0 , or D^{*+} and X is a system consisting of up to five particles of the type π^\pm, π^0, K^\pm , or K_S^0 [11]. D^{*+} mesons are reconstructed in the channel $D^0\pi^+$. D^0 mesons are reconstructed in the channels $K^-\pi^+$, $K^-\pi^+\pi^0$, $K^-\pi^+\pi^-\pi^+$, and $K_S^0\pi^+\pi^-$. D^+ mesons are reconstructed in the channels $K_S^0\pi^+$, $K^-\pi^+\pi^+$, $K_S^0\pi^+\pi^0$, $K_S^0\pi^+\pi^+\pi^-$, and $K^+K^-\pi^+$. The ΔE of the companion B is required to be within two mode-dependent standard deviations of the mean when no π^0 is present, or to satisfy $-0.09 < \Delta E < 0.06$ GeV for reconstructions with one or more π^0 . If more than one B candidate is reconstructed in the same mode, the reconstructed B with the smallest $|\Delta E|$ is selected. For each mode, the purity B_{pur} is the ratio of the number of events before signal selection in the fitted peak to the total number of events in the region $5.27 < m_{\text{ES}} < 5.29$ GeV. Only events reconstructed in a mode with $B_{\text{pur}} > 0.12$ are selected, which results in the reconstruction of 147 distinct modes in the data sample. If B candidates are reconstructed in more than one mode, the B reconstructed in the mode with the highest B_{pur} is selected as the companion B .

We estimate the total companion- B yield from all reconstructed modes using the $B\bar{B}$ and $q\bar{q}$ ($q = u, d, s, c$) simulated samples before applying the signal $B^0 \rightarrow \tau^+\tau^-$ selection. We first remove the peak from the $B^0\bar{B}^0$ simulated sample using the fitted Crystal Ball probability density function. Subtracting the simulated combinatorial background m_{ES} shape, fitted to the data below 5.26 GeV, from the data distribution yields a nominal companion- B yield of $N_{B^0\bar{B}^0} = (2.80 \pm 0.27) \times 10^5$ (Fig. 2). The systematic error on $N_{B^0\bar{B}^0}$ is estimated to be 10% by varying the fit region and by varying the combinatorial background composition with event-shape-variable cuts.

The companion- B decay products are removed from the event and the signal- B characteristics are sought among the remaining particles. The dominant background to $B^0 \rightarrow \tau^+\tau^-$ arises from decays $b \rightarrow W^-c(\rightarrow W^+s)$, in which the s quark hadronizes into a K_L^0 that escapes detection and the virtual W^+ and W^- mimic

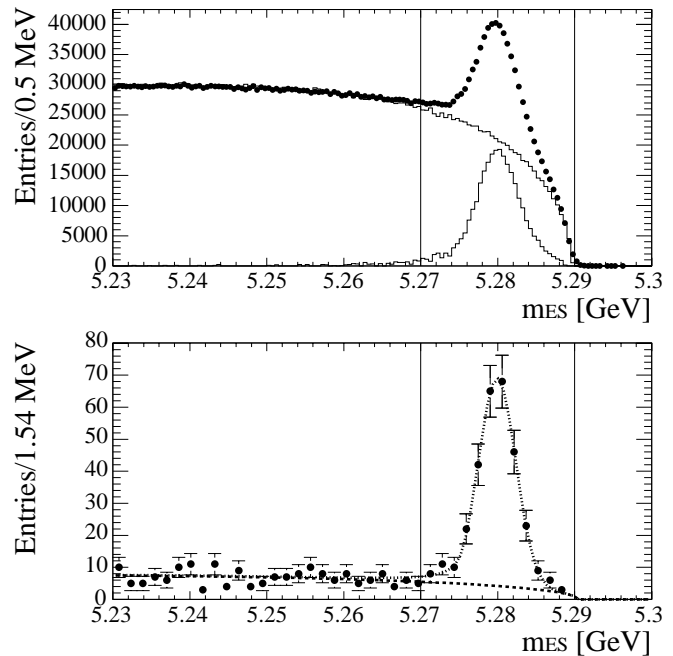


FIG. 2: Above, the m_{ES} distribution for the hadronic companion B in data (dots) and scaled simulated background (upper histogram) before the signal $B^0 \rightarrow \tau^+\tau^-$ selection is applied; the lower histogram is obtained by subtracting the background from the data. The companion- B yield is $N_{B^0\bar{B}^0} = (2.80 \pm 0.27) \times 10^5$. Below, the m_{ES} distribution after the signal $B^0 \rightarrow \tau^+\tau^-$ selection. The fitted probability density function (short-dash) and its ARGUS component (dash) are superimposed on the data (dots). We obtain $N_{\text{obs}} = 263 \pm 19$ events in the peak.

the virtual W^+ and W^- emitted by the signal τ . A secondary background originates in events in which two oppositely charged particles are lost outside the detector fiducial region. We select signal events that are consistent with each τ decaying to a single charged particle (and one or two ν) by selecting events with zero net charge and two tracks in the recoil system. Each track must leave at least twelve hits in the DCH, originate within 10 cm of the beamspot in the beam direction and within 1.5 cm in the transverse direction, and have a transverse momentum of at least 0.1 GeV. To eliminate background originating from $b \rightarrow W^-c(\rightarrow W^+s)$ events, the selection rejects events with identified K^+ , K_S^0 , or K_L^0 . The K^\pm candidates are identified by a neural network with inputs taken from the SVT, the DCH, and the DIRC. The K_S^0 candidates are identified as a $\pi^+\pi^-$ pair with invariant mass consistent with the K_S^0 mass ($0.473 < m_{\pi^+\pi^-} < 0.523$ GeV). The K_L^0 candidates are identified from clusters in the EMC that have not been associated with a charged track or included in a candidate π^0 . A neural network is employed to identify K_L^0 candidates using the cluster energy and shower-shape variables, which discriminate hadronic from electromag-

TABLE I: Signal $B^0 \rightarrow \tau^+\tau^-$ branching fraction and requirements by mode ($\ell = e, \mu$).

Selection Mode	$\mathcal{B}(\%)$ [12]	$N_e + N_\mu$	N_{π^0}	$m_{\pi\pi^0}$
$\tau^+\tau^- \rightarrow \ell\nu\bar{\nu}/\ell'\nu\bar{\nu}$	12.4	2	0	NA
$\tau^+\tau^- \rightarrow \ell\nu\bar{\nu}/\pi\nu$	7.8	1	0	NA
$\tau^+\tau^- \rightarrow \ell\nu\bar{\nu}/\rho\nu$	17.7	1	1	[0.6, 1.0] GeV
$\tau^+\tau^- \rightarrow \pi\nu/\pi\nu$	1.2	0	0	NA
$\tau^+\tau^- \rightarrow \pi\nu/\rho\nu$	5.6	0	1	[0.6, 1.0] GeV
$\tau^+\tau^- \rightarrow \rho\nu/\rho\nu$	6.3	0	2	[0.6, 1.0] GeV

TABLE II: ϵ_{sig} , $N_{expected}$ and N_{obs} obtained from individual fits by signal mode. The errors are statistical and fit error added in quadrature. Branching fractions are included in the efficiency estimates. The $\pi\nu/\pi\nu$ channel is dominated by crossfeed from other signal channels.

Selection Mode	$\epsilon_{sig}(\%)$	$N_{expected}$	N_{obs}
$\tau^+\tau^- \rightarrow \ell\nu\bar{\nu}/\ell'\nu\bar{\nu}$	0.9 ± 0.2	46 ± 4	54 ± 7
$\tau^+\tau^- \rightarrow \ell\nu\bar{\nu}/\pi\nu$	1.5 ± 0.3	122 ± 6	105 ± 11
$\tau^+\tau^- \rightarrow \pi\nu/\pi\nu$	1.5 ± 0.3	89 ± 6	80 ± 11
$\tau^+\tau^- \rightarrow \rho\nu/\rho\nu$	0.3 ± 0.1	21 ± 3	15 ± 6

netic showers.

The multiplicities of e , μ , and π^0 in the recoil system must be consistent with each τ decaying in one of the channels $\tau \rightarrow \pi\nu, \rho\nu, e\nu\bar{\nu}$ or $\mu\nu\bar{\nu}$ (Table I). The e candidates are identified with dE/dx measurements from the DCH and shower shape variables from the EMC. The μ candidates are identified with variables from the IFR (to reject the π hypothesis) and EMC (to reject the e hypothesis). Track candidates that are not identified as e , μ or K are assumed to be π . Events with π^0 are vetoed unless the π^0 can be associated to a π^+ such that the invariant mass is consistent with the ρ mass ($0.6 < m_{\pi^+\pi^0} < 1.0$ GeV). The π^0 candidates are formed from pairs of γ candidates with invariant mass $0.090 < m_{\gamma\gamma} < 0.170$ GeV, with each γ having an energy greater than 0.030 GeV. Since the presence of residual unassociated energy in the EMC (E_{res}) is a strong indication that an unreconstructed π^0 or K^0 is present, we require $E_{res} < 0.11$ GeV.

The τ -daughter candidates are Lorentz-boosted with the companion- B momentum. While distributions of the momenta \mathbf{p}_+ and \mathbf{p}_- of the charged daughters exhibit no discrimination from the background momentum distributions, correlations among $|\mathbf{p}_+|$, $|\mathbf{p}_-|$, and $\cos\theta \equiv \mathbf{p}_+ \cdot \mathbf{p}_- / |\mathbf{p}_+||\mathbf{p}_-|$ afford some discrimination, especially when categorized by signal $B^0 \rightarrow \tau^+\tau^-$ selection mode. Cascade decay background events manifest an asymmetry in $|\mathbf{p}_+|$ and $|\mathbf{p}_-|$ that is not present in signal events. The parameters $|\mathbf{p}_+|$, $|\mathbf{p}_-|$, $\cos\theta$, E_{res} , and the selection mode are used as inputs in a neural-network analysis trained to discriminate signal from background.

The final selection requirement is a neural network output (NN) consistent with signal events.

The signal $B^0 \rightarrow \tau^+\tau^-$ selection criteria for E_{res} , NN and B_{pur} are chosen to minimize the expected upper limit on $\mathcal{B}(B^0 \rightarrow \tau^+\tau^-)$. That optimization also rejects the signal selection modes $\tau^+\tau^- \rightarrow \ell\nu\bar{\nu}/\rho\nu$ and $\tau^+\tau^- \rightarrow \pi\nu/\rho\nu$. After the full signal $B^0 \rightarrow \tau^+\tau^-$ selection, the combinatorial companion- B background is estimated and subtracted using ARGUS and Crystal Ball fits to the m_{ES} distributions in simulation samples and data (Fig. 2). From these fits we determine the signal efficiency (ϵ_{sig}), the expected number of background events ($N_{expected}$), and the number of observed data events (N_{obs}). Including systematic uncertainties described below, we obtain $\epsilon_{sig} = 0.043 \pm 0.009$, and $N_{expected} = 281 \pm 48$. We extract from the fit $N_{obs} = 263 \pm 19$ events in the data after the full selection. The central value of the $B^0 \rightarrow \tau^+\tau^-$ branching fraction is $(-1.5 \pm 4.4) \times 10^{-3}$. We find no evidence for signal events. Table II shows ϵ_{sig} , $N_{expected}$ and N_{obs} obtained from individual fits to specific signal selection modes.

Systematic uncertainties on $N_{expected}$ and ϵ_{sig} arise from several sources. The simulation statistical uncertainty for $N_{expected}$ (ϵ_{sig}) is 10 events (11%). The systematic uncertainties are estimated for cluster corrections to be 8 (3%), for particle identification corrections 10 (10%), and for tracking corrections 7 (3%). The m_{ES} background subtraction fits after the full selection add a further systematic uncertainty of 4 (2%). We estimate the systematic uncertainty on $N_{expected}$ due to B decay modeling in EvtGen to be 10%. We estimate the systematic uncertainty due to our model of τ decay by inserting distributions obtained from the specialized τ Monte Carlo TAUOLA [13] to decay two τ produced with the same helicity and the requisite momentum for a $B^0 \rightarrow \tau^+\tau^-$ decay. For each simulated event, the decay mode of each τ is identified and the $|\mathbf{p}_+|$, $|\mathbf{p}_-|$ and $\cos\theta$ values are replaced with values sampled from distributions generated by TAUOLA for that mode. The relative ϵ_{sig} variation between EvtGen and TAUOLA simulation is 2%.

A final systematic uncertainty for both signal and background is assigned to the modeling of E_{res} . The simulation of background hits and hadronic interactions in the EMC does not perfectly model the data, and the discrepancy manifests itself in the E_{res} distribution (Fig. 3). This uncertainty is estimated from the difference between data and the simulation for a control process. The control sample selection is identical to the $B^0 \rightarrow \tau^+\tau^-$ selection except that events with an additional reconstructed K_S^0 are selected and the K_S^0 daughters are removed from the event. For correct K_S^0 reconstructions, this control sample models the K_L^0 background while for K_S^0 reconstructions from random combinations of tracks it models the backgrounds in which two oppositely charged particles are lost due to the limited detector acceptance in the direction of the higher energy beam. The compo-

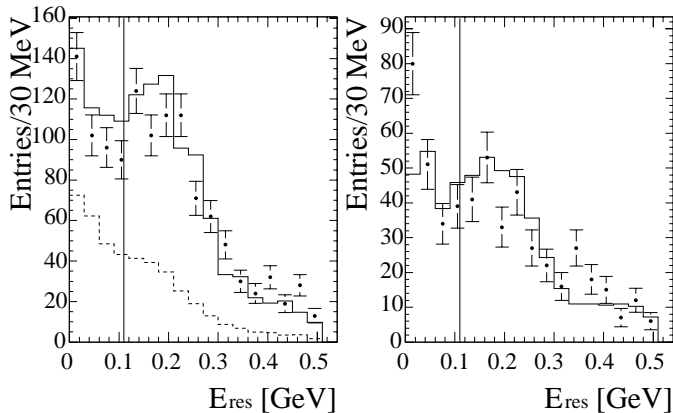


FIG. 3: The E_{res} distribution in the nominal sample (left) and the control sample (right) for data (dots), simulated background (solid histogram), and simulated signal (dashed histogram). The simulated signal distribution normalization is arbitrary. All requirements except those for E_{res} and NN are imposed. The events to the left of the vertical line are selected.

sition of the background in the simulated control sample agrees well with that of the simulated signal sample. The control sample yields are 135 ± 14 events (data) and 125 ± 7 (simulation), for a relative discrepancy of $(8 \pm 13)\%$, consistent with zero. The systematic uncertainty due to modeling the residual energy in the EMC is taken to be the uncertainties in data and simulation yields added in quadrature, namely 13%.

Systematic uncertainties on the companion- B yield, expected background, and ϵ_{sig} are folded into the upper limit calculation using the technique described in Ref. [14], giving

$$\mathcal{B}(B^0 \rightarrow \tau^+\tau^-) < 4.1 \times 10^{-3}, \quad (4)$$

at the 90% confidence level. The result constrains leptoquark couplings as described in Ref. [2]. For example, the scalar $SU(2)$ doublet leptoquark $S_{1/2}$ can mediate $B^0 \rightarrow \tau^+\tau^-$. If no other leptoquark mediates the decay, the product of its coupling λ_R^{33} (coupling righthanded b with τ) with λ_R^{13} (coupling righthanded d with τ) is

$$\lambda_R^{33}\lambda_R^{13} < 1.4 \times 10^{-2} \left[\frac{m_{S_{1/2}}}{100 \text{ GeV}} \right]^2, \quad (5)$$

at the 90% confidence level, where $m_{S_{1/2}}$ is the $S_{1/2}$ mass.

We are grateful for the excellent luminosity and machine conditions provided by our PEP-II colleagues, and for the substantial dedicated effort from the computing organizations that support *BABAR*. The collaborating institutions wish to thank SLAC for its support and kind hospitality. This work is supported by DOE and NSF (USA), NSERC (Canada), IHEP (China), CEA and CNRS-IN2P3 (France), BMBF and DFG (Germany), INFN (Italy), FOM (The Netherlands), NFR (Norway), MIST (Russia), and PPARC (United Kingdom). Individuals have received support from CONACyT (Mexico), A. P. Sloan Foundation, Research Corporation, and Alexander von Humboldt Foundation.

* Also with University of California at San Diego, La Jolla, CA 92093, USA

- [1] P. Harrison and H. Quinn, Tech. Rep. SLAC-R-504, SLAC (1998).
- [2] Y. Grossman, Z. Ligeti, and E. Nardi, Phys. Rev. **D55**, 2768 (1997).
- [3] H. E. Logan and U. Nierste, Nucl. Phys. **B586**, 39 (2000).
- [4] K. Babu and C. Kolda, Phys. Rev. Lett. **84**, 241802 (2000).
- [5] B. Aubert et al. (The *BABAR* Collaboration), Nucl. Instrum. Meth. A **479**, 1 (2002).
- [6] D. Lange, Nucl. Instrum. Meth. A **462**, 152 (2001).
- [7] S. Agostinelli et al. (The GEANT Collaboration), Nucl. Instrum. Meth. A **506**, 250 (2003).
- [8] The Crystal Ball function is defined to be
$$X(m) = \begin{cases} (1 + \alpha(m - m_0)/n\sigma - \alpha^2/n)^{-n} \exp[-\frac{1}{2}\alpha^2] \\ \exp[-(m - m_0)^2/2\sigma^2] \end{cases}$$
 for $(m - m_0) < \sigma\alpha$ (top) and $(m - m_0) \geq \sigma\alpha$ (bottom).
- [9] The ARGUS function is defined to be
$$A(m) = m\sqrt{1 - (m/m_c)^2} \exp[a(1 - (m/m_c)^2)].$$
- [10] Charge conjugate states are included implicitly throughout this paper.
- [11] B. Aubert et al. (The *BABAR* Collaboration), Phys. Rev. Lett. **92**, 071802 (2004).
- [12] S. Eidelman et al., Phys. Lett. **B592**, 1 (2004).
- [13] P. Golonka, B. Kersevan, T. Pierzchala, E. Richter-Was, Z. Was, and M. Worek, submitted to Comput. Phys. Commun. (2003), hep-ph/0312240v1.
- [14] R. Barlow, Comput. Phys. Commun. **149**, 97 (2002).